Macromolecules
ARTICLE

*Macromolecules* **2009**, *42*, 9457–9466 **9457**
DOI: 10.1021/ma902115j

# Monitoring Block-Copolymer Crossover-Chemistry in ROMP: Catalyst Evaluation via Mass-Spectrometry (MALDI)

**Wolfgang H. Binder,* Bhanuprathap Pulamagatta, Onur Kir, Steffen Kurzhals, Haitham Barqawi, and Susanne Tanner**

*Chair of Macromolecular Chemistry, Institute of Chemistry, Faculty of Natural Sciences II (Chemistry and Physics), Martin-Luther Universität Halle-Wittenberg D-06120 Halle, Germany*

*Received July 6, 2009; Revised Manuscript Received November 9, 2009*

ABSTRACT: We report on the monitoring and evaluation of the crossover reaction in ring-opening metathesis polymerization (ROMP) via MALDI methods. ROMP of various monomers using several catalytic systems (first-generation (**I**) and third-generation Grubbs-type (**III**)) was investigated with structurally different norbornene monomers derived from (±)*endo*,*exo*-bicyclo[2,2,1]-hept-5-ene-2,3-dicarboxylic acid-bis-*O*-methyl ester (monomer **A**), (±)*endo*,*exo*-bicyclo[2,2,1]-hept-5-ene-2,3-dicarboxylic acid-bis-*O*-2,2,6,6-tetramethyl piperidinoxyl-ester (monomer **T**), (±)*exo*-*N*-(4,4,5,5,6,6,7,7,7-nonafluoroheptyl)-10-oxa-4-azatricyclodec-8-ene-3,5-dione (monomer **D**), and the highly strained monomer 2-methyl-2-phenyl-cyclopropene (monomer **E**). The crossover reactions as well as the polymerization kinetics of the various monomers were studied in detail, in particular, using matrix-assisted laser desorption ionization mass spectrometry (MALDI). Catalyst **III** offered access to the synthesis of highly defined block copolymers, generating poly(**A**-*b*-**T**), poly(**A**-*b*-**D**), and poly(**A**-*b*-**E**) diblockcopolymers in high precision, whereas catalyst **I** offered access to the diblockcopolymers poly(**A**-*b*-**D**) and poly(**A**-*b*-**E**). Poly(**A**) was used as a probe to analyze the crossover reaction, revealing well-defined crossover kinetics in the case of monomers **T**, **D**, and **E** and a subsequent good polymerization after the crossover reaction in the case of monomer **E**. The presented system allows a simple evaluation and monitoring of crossover reactions in ROMP-based polymerization reactions.

## Introduction

Ring-opening metathesis polymerization (ROMP) is now established as a powerful tool for the preparation of homo and block copolymers, enabling a large variety of monomers to be polymerized up to molecular weights of several 100 000 g mol$^{-1}$ with nearly freely adjustable block ratios.[1−7] According to the classical rules for a living polymerization,[8] the achievement of a successful block copolymerization of monomers via ROMP is linked to critical parameters such as (a) the optimization of the optimal monomer/catalyst combination, (b) the maintenance of livingness of the active species throughout the polymerization reaction, (c) avoiding backbiting reactions[9] and thus reducing the loss of already polymerized monomers from the chains in the form of cycles, (d) achieving fast initiation in relation to propagation (i.e., $k_i > k_p$), and (e) avoiding chain transfer reactions.[8] In particular, the quest of an appropriate monomer/catalyst combination often proves to be difficult because even structurally related monomers often cannot be polymerized equally well with the same type of catalyst, thus leading to poor crossover reactions, broader polydispersities, and less-defined molecular weights. Unfortunately, many of the above-mentioned issues are complicated by complex ligand catalyst equilibria,[10,11] leading to large differences in the reactivity of the propagating species during the crossover reaction. With the advent of Grubb's first-, second-, and third-generation catalysts,[12] a set of relatively stable, commercially available, and kinetically highly diverse catalytic systems have become available, whose reactivity can be tuned by the use of additional additives such as acids, solvents, or nitrogen-based bases. Often, steric concepts in catalyst design are used to direct block copolymerization reactions by purely controlling available space around the catalyst species.[13,14] Systematic steric effects resulting from the ROMP of dendritic monomers have been described, resulting in autoinhibition due to polymer interaction with the catalyst.[15] However, the underlying crossover reactions often rely on the direct analysis of block-copolymerization reactions with respect to $M_n$, $M_w/M_n$ (via GPC), or the corresponding block ratio (via NMR) without any knowledge of the intermediate species during the crossover process in the case of poor or insufficient polymerization results. Studies by Chen et al.[16−18] have been conducted by ESI-MS; however, they are limited to highly charged monomers because of the selective ionization process in ESI-TOF mass spectrometry.

The following article investigates the crossover reactions of four structurally different monomers in a ROMP-based block copolymerization via (a) kinetic analysis and (b) MALDI mass spectrometry. The monomers chosen (monomers **A**, **T**, **D**, and **E**) (Scheme 1) display their best ROMP processes with different catalysts (first- (**I**), second- (**II**), and third-generation (**III**) Grubbs type) such as monomers **A** and **D** with catalyst Grubbs first-generation,[19] monomer **T** with Grubbs second-generation,[20] and monomer **E** with Grubbs second- and third-generation catalysts.[21] Whereas the classical kinetic analysis enables the qualitative monitoring of the chain-growth reaction of the ROMP process, MALDI mass spectrometric methods allows the monitoring of the reaction directly at the point of the crossover reaction, thus enabling a better evaluation of the polymerization directly at the crossover reaction.

*Corresponding author. E-mail: wolfgang.binder@chemie.uni-halle.de.

© 2009 American Chemical Society

Published on Web 11/19/2009

**Scheme 1. Monomers and Catalysts Used for the Crossover Reactions**

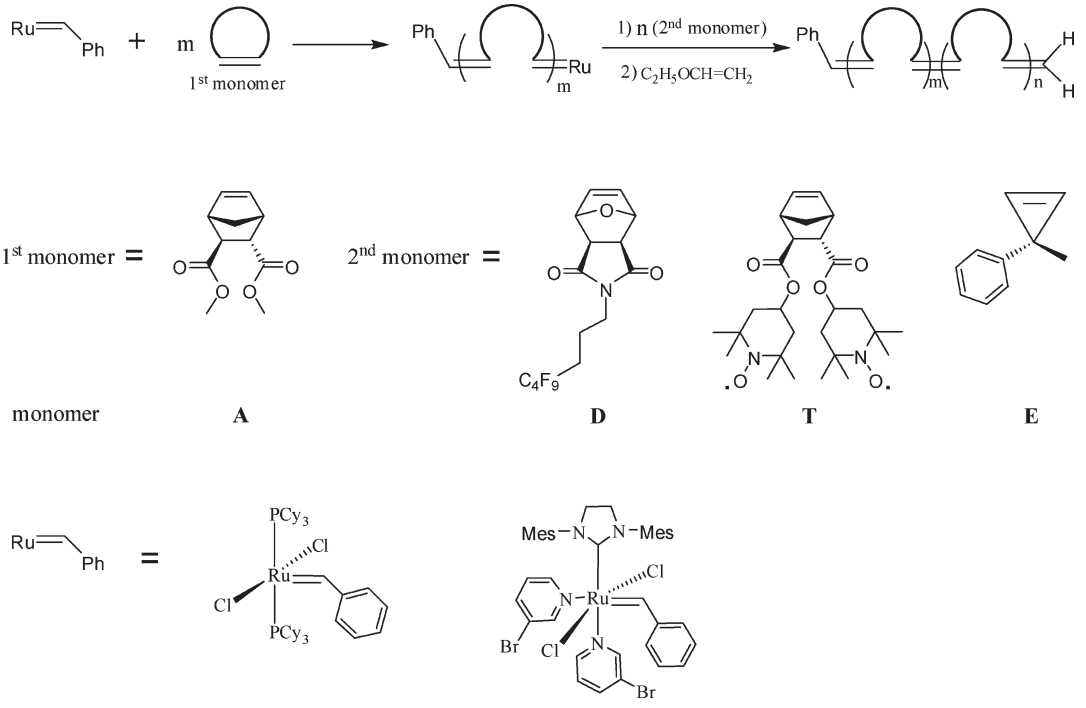


## Experimental Section

**Instrumentation.** $^1$H NMR spectra were performed on a Varian Gemini 200 or 400 MHz FT-NMR spectrometer, and MestRec (4.9.9.9) was used for data interpretation. The polymerization kinetics of the homo and block copolymerization reactions with both catalysts **I** and **III** were measured at 25 °C on a 200 MHz FT-NMR spectrometer using $CDCl_3$ as a solvent. GPC analysis was done on a Viscotek VE2001 system using THF as an eluent with a flow rate of 1 mL/min and injection volume of 100 $\mu$L. Polystyrene standards were used for conventional external calibration using a Viscotek VE3580 refractive index detector. Positive ion MALDI-TOF (matrix-assisted laser desorption ionization time-of-flight) measurements were performed on Bruker Autoflex-III instrument equipped with a smart ion beam laser. Measurements were carried out in linear and reflector mode. Samples were prepared from THF solution by mixing matrix (20 mg/mL), polymer (20 mg/mL), and salt (20 mg/mL solution) in a ratio of 100:10:1. Dithranol (1,8-dihydroxy-9(10*H*)-anthracetone, Aldrich 97%) was used as the matrix. Sodium trifluoroacetate (Aldrich, 98%) or silver trifluoroacetate (Aldrich, 99.99%) or lithium trifluoroacetate (Aldrich, 99.8%) salts were added for ion formation, with sodium trifluoroacetate used as the optimal salt for obtaining the highest S/N ratio.

**Solvents/Reagents/Materials.** Catalysts **I** and **III** were obtained from Sigma-Aldrich. Dichloromethane ($CH_2Cl_2$) and dimethylformamide (DMF) were freshly distilled over $CaH_2$ and degassed with argon prior to use. The other solvents such as petrolether, ethyl acetate, and hexane were used after distillation. All other reagents were purchased from Sigma Aldrich (Germany) and were used without further purification. *endo*, *exo*-Bicyclo[2,2,1]-hept-5-ene-2,3-dicarboxylic acid dimethylester (monomer **A**) was prepared according to modified procedure from ref 19; *endo*,*exo*-bicyclo[2,2,1]-hept-5-ene-2,3-dicarboxylic acid-bis-*O*-2,2,6,6-tetramethyl piperidinoxyl-ester (monomer **T**) was prepared according to refs 20 and 22; *exo*-*N*-(4,4,5,5,6,6,7,7,7-nonafluoroheptyl)-10-oxa-4-azatricyclodec-8-ene-3,5-dione (monomer **D**) was prepared in a two-step procedure (described below); and 3-methyl-3-phenylcyclopropene (monomer **E**)[21,23] was prepared according to literature procedures.

**Synthesis of *endo*,*exo*[2.2.1] Bicyclo-2-ene-5,6-dicarboxylic Acid Dimethylester (Monomer A).** A modified literature synthesis[19] was adopted, and thus methanol (3.1 g, 94.9 mmol) and pyridine (7.5 g, 95.2 mmol) were dissolved in 60 mL of dry $CH_2Cl_2$. Under ice cooling, *endo*,*exo*[2.2.1] bicyclo-2-ene-5,6-dicarboxylic acid chloride (5.2 g, 23.8 mmol) was dropped into the reaction mixture and stirred overnight at room temperature. The reaction mixture was filtered to remove the pyridinium salt and extracted with $CH_2Cl_2$. The organic layer was extracted with 2 N HCl solution and saturated sodium bicarbonate and dried with sodium sulfate. The solvent was removed under reduced pressure. Finally, the product was purified using column chromatography with petrolether/ethyl acetate (10:1) as the solvent mixture to yield 3.9 g (78%) of monomer **A** as a white solid. All NMR data were in accordance with literature values.[19] $^1$H NMR ($\delta$, $CDCl_3$, 400 MHz): 6.27 (q, 1H), 6.07 (q, 1H), 3.71 (s, 3H), 3.64 (s, 3H), 3.37 (t, 1H), 3.26 (s, 1H), 3.13 (s, 1H), 2.68 (m, 1H), 1.60 (m, 1H), 1.47 (m, 1H).

**Synthesis of Exo-*N*-(4,4,5,5,6,6,7,7,7-nonafluoroheptyl)-10-oxa-4-azatricyclodec-8-ene-3,5-dione (Monomer D).** The synthetic procedure was adopted from ref 24. Freshly distilled furan (15 mL, 207.1 mmol) and maleimide (2 g, 20.6 mmol) were placed in a 100 mL large autoclave equipped with heating bath. The mixture was stirred at 90 °C under an argon atmosphere for 10 h. The reaction vessel was cooled to RT to regain atmospheric pressure, whereupon white crystals precipitated. The white precipitate was collected by vacuum filtration and washed two times with furan. The white precipitate was further dried under high vacuum overnight to yield 3.3 g (96%) of pure and dry exo-10-oxa-4-aza-tricyclo-dec-8-ene-3,5-dione. All NMR data were in accordance with literature values.[24] $^1$H NMR ($\delta$, 400 MHz, DMSO): 11.09 (s, 1H), 6.48 (s, 2H), 5.07 (s, 2H), 2.83 (s, 2H).

A solution of 4,4,5,5,6,6,7,7,7-nonafluoro-heptan-1-ol (1.0 g, 3.60 mmol) and tetrabromomethane (1.878 g, 5.663 mmol) in dry $CH_2Cl_2$ (20 mL) was cooled to 0 °C, and a solution of triphenylphosphine (1.415 g, 5.393 mmol) in dry $CH_2Cl_2$ (5 mL) was slowly added. The ice bath was removed, and the mixture

was stirred for 12 h at ambient temperature. After complete conversion, the solvent was removed under reduced pressure (care was taken not to remove the intermediate 7-bromo-1,1,1,2,2,3,3,4,4-nonafluoroheptane from the reaction mixture under reduced pressure), and the crude product was subsequently reacted without any further purification. Potassium carbonate (1.098 g, 7.910 mmol) and exo-10-oxa-4-azatricyclodec-8-ene-3,5-dione (0.653 g, 3.955 mmol) was added to the crude 7-bromo-1,1,1,2,2,3,3,4,4-nonafluoroheptane and resuspended in dry DMF (60 mL). The reaction mixture was stirred for 24 h at ambient temperature, and the solvent was subsequently removed under reduced pressure. The obtained crude compound was dissolved in $CH_2Cl_2$ and extracted with water and dried, and, subsequently, the $CH_2Cl_2$ was removed under reduced pressure. Finally, the product was purified by chromatography ($SiO_2$, hexane/ethyl acetate 1/1) to yield 1.0 g (61%) of pure white crystals of monomer **D**. All NMR data were in accordance with literature values.[24] $^1$H NMR ($\delta$, 400 MHz, $CDCl_3$): 6.51 (td, $J$ = 4.42, 0.80, 0.80 Hz, 2H), 5.26 (td, $J$ = 1.87, 0.90, 0.90 Hz, 2H), 3.57 (t, $J$ = 6.92, 6.92 Hz, 2H), 2.88−2.83 (m, 2H), 2.14−1.97 (m, 2H), 1.95−1.83 (m, 2H).

**Synthesis of Poly($\mathbf{A_{100}}$).** A heated and argon-flushed glass tube equipped with a magnetic stirbar was charged with monomer **A** (83.0 mg, 0.39 mmol) in 1 mL of $CH_2Cl_2$. To this solution was added catalyst **I** (3.3 mg, 0.004 mmol) dissolved in 1 mL of $CH_2Cl_2$. The reaction mixture was stirred for 4 h at room temperature until all of monomer **A** was consumed, as checked by thin layer chromatography (TLC). The reaction was then quenched with cold ethyl vinyl ether, and the resulting polymer was precipitated into cold methanol (300 mL). The methanol was decanted, and the product was dried under high vacuum overnight to yield 80 mg (96%) of poly(**A**). The polymerization of monomer **A** with catalyst **III** was carried out in the same manner but with the polymerization time of 1 h because of the faster reaction. Poly($\mathbf{A}$)$_n$ with different chain lengths ($n$ = 15, 25, 50) with both catalysts **I** and **III** was also prepared using the same procedure by adopting the required polymerization times.

**Block Copolymer Syntheses.** The synthesis of block copolymers poly($\mathbf{A}_n$-*b*-$\mathbf{D}_m$), poly($\mathbf{A}_n$-*b*-$\mathbf{T}_m$), and poly($\mathbf{A}_n$-*b*-$\mathbf{E}_m$) was done analogously to methods developed previously in our laboratory.[24−27] The synthesis given below is indicative of the methods used for the preparation of all block copolymers.

*General Synthesis Procedure of Block Copolymerization*. For example, the synthesis for poly($\mathbf{A}_{25}$-*b*-$\mathbf{D}_{25}$) is given below: monomer **A** (33.1 mg, 0.16 mmol) in 0.5 mL of $CH_2Cl_2$ was added to the catalyst **I** (Grubbs first-generation, $RuCl_2(PCy_3)_2$-(CHPh)) (5.18 mg, 0.006 mmol) dissolved in 1 mL of $CH_2Cl_2$ in a heated and argon-flushed glass vial equipped with a magnetic stir bar. The polymerization was carried out at room temperature for 1 h until all of monomer **A** was consumed, as checked by NMR and TLC. Monomer **D** (66.9 mg, 0.16 mmol) as a solution in 0.5 mL of $CH_2Cl_2$ was then added to the above reaction mixture and stirred for 1 h at room temperature until all of monomer **D** was consumed, as checked by NMR and TLC. The polymerization was quenched by the addition of cold ethyl vinyl ether. The produced polymer was isolated by precipitating in cold methanol, or alternatively, the polymer was isolated by column chromatography ($SiO_2$). Finally, the product was dried under high vacuum overnight to yield 97 mg (97%) of poly($\mathbf{A}_{25}$-*b*-$\mathbf{D}_{25}$). The other block copolymers, poly($\mathbf{A}_n$-*b*-$\mathbf{T}_m$) and poly($\mathbf{A}_n$-*b*-$\mathbf{E}_m$), with catalysts **I** and **III** were synthesized using the above stated procedure but adopting the different reaction times according to the kinetic data.

*Kinetic Experiments*. A pyrene stock solution was prepared from 70 mg of pyrene dissolved in 2 mL of $CDCl_3$. The NMR tube was filled with the first monomer (i.e., monomer **A**, 17 mg) dissolved in $CDCl_3$ (0.2 mL) and pyrene stock solution (0.2 mL). Before adding the initiator solution, the ratio of the monomer to the internal standard was determined by NMR. On the basis of this value, the monomer concentration at $t$ = 0 was determined. A solution of the initiator in $CDCl_3$ ([c] $\approx$ 3.3 mg in 0.2 mL of $CDCl_3$) was added via a syringe to yield the desired monomer to initiator ratio. After shaking, the tube was inserted into the NMR spectrometer, and the decrease in the monomer versus time was monitored. The second monomer (i.e., monomer **D**, 33 mg) dissolved in $CDCl_3$ (0.2 mL) was added after complete conversion of the first monomer. For determination of the monomer concentration at $t$ = 0 and the monomer consumption, the corresponding signals were integrated: signals at 6.27 and 6.07 ppm (2H) for monomer **A**, the signal at 6.50 ppm (2H) for monomer **D**, and the signal at 1.64 ppm (3H) monomer **E** was compared with the one at 8.20 ppm (4H, d, CH) from the internal standard pyrene. The time between the addition of the initiator solution and the first measurement was added to the first measuring point.

## Results and Discussion

**Polymerization.** To study the crossover reactions of different monomers, structurally different monomers **A**, **D**, **T**, and **E** (Scheme 1) were chosen and prepared.[19−21] Therefore, monomers **A**, **D**, and **T** are related in their norbornene/oxynorbornene structure; however, they bear structurally largely different substituents. Therefore, monomer **A** carries two carboxymethyl moieties, monomer **D** carries a perfluoroalkyl−maleimide moiety, and monomer **T** carries two nitroxide moieties. Monomer **E** is characterized by a cyclopropene moiety with a comparably high ring strain. As described by us[21] and others,[20] the optimal polymerization of the monomers is characterized by different Ru-based catalysts; therefore, monomers **A** and **D** are characterized by Grubbs first-generation catalyst,[19] monomer **T** is characterized by Grubbs second-generation catalyst,[20] and monomer **E** is characterized by Grubbs second- and third-generation catalysts.[21] The crossover reactions were investigated using monomer **A** as the first monomer and then crossing over to the other monomers **D**, **T**, or **E**. The reason for this choice was the excellent desorption of homopolymer poly($\mathbf{A}$)$_n$ (i.e., $\mathbf{A}_{15}$ or $\mathbf{A}_{20}$) via MALDI methods, thus opening the chance to monitor the crossover reaction directly via the MALDI-methods (vide infra).

Polymerization reactions were conducted using Grubbs first- (**I**) and third-generation (**III**) catalyst. Grubbs second-generation (**II**) catalyst was not further investigated because monomer **A** is only poorly polymerized with this catalyst (data not shown). The kinetic features of the polymerization reactions were first analyzed via $M_n$ versus time graphs (as measured by GPC with the monomers **A**−**D**, **A**−**T**, and **A**−**E**). The crossover data are shown in Figures 1 and 2. Figure 1 shows the homopolymerization of monomer **A** with catalysts **I** and **III** (Figure 1a,c) and the crossover reactions from living poly(**A**) to monomer **D** (Figure 1c) and monomer **T** (Figure 1d). Both reactions are well controlled, clearly demonstrating an efficient crossover reaction between these monomers. GPC data for the crossover reactions are shown in Table 1, indicating the efficiency of this process, with $M_w/M_n$ values ranging from 1.1 to 1.25. A similar picture is observed when studying the crossover reaction from monomers **A** to **E** using Grubbs first- and third-generation catalysts. (See Figure 2a,b.) In both cases, a significant change in the kinetics before and after the crossover point can be seen because chain growth of monomer **E** is significantly slower than that with monomer **A** with both catalysts.

This prompted us to study kinetics before and after the crossover reactions, as monitored by $^1$H NMR spectroscopy (Supporting Information), directly obtaining the $\ln(M_o/M_t)$ graphs versus time ($t$). Because monomer **T** represents a free radical, its kinetics could not be investigated by $^1$H NMR

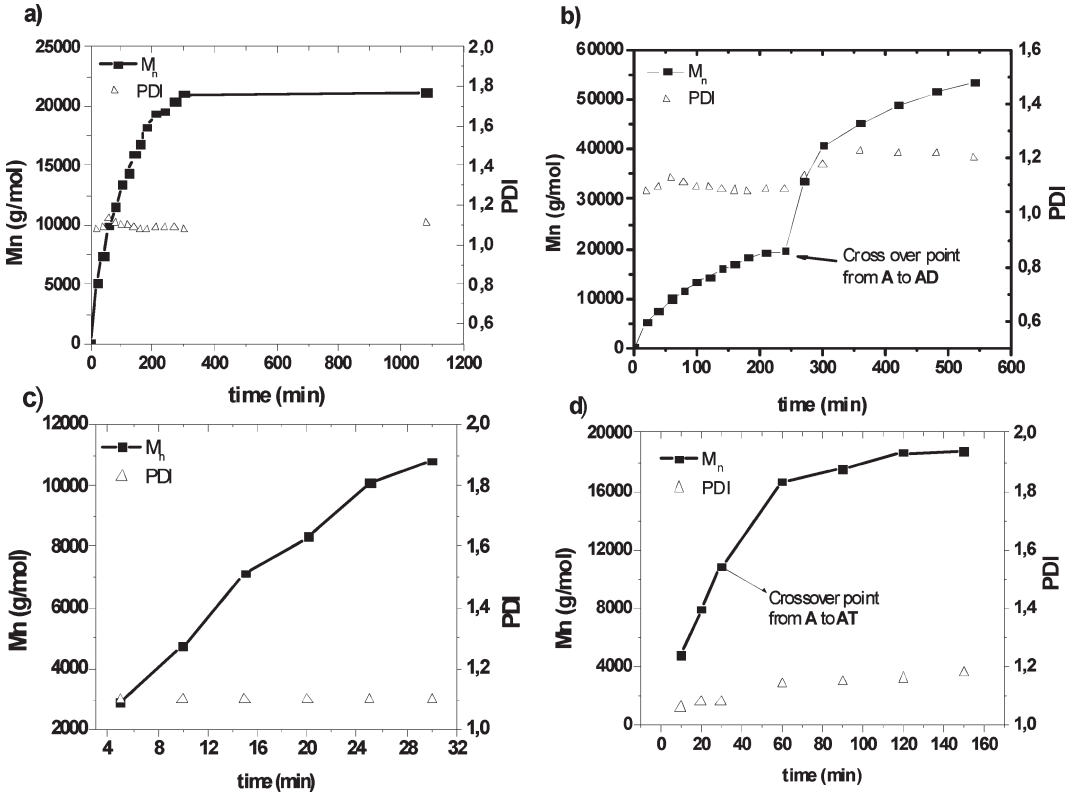


**Figure 1.** Increase in $M_{n(GPC)}$ with polymerization time ($t$) for (a) poly($\mathbf{A}_{100}$) and (b) poly($\mathbf{A}_{100}$-*b*-$\mathbf{D}_{100}$) using catalyst **I** and for (c) poly($\mathbf{A}_{50}$) and (d) poly($\mathbf{A}_{50}$-*b*-$\mathbf{T}_{20}$) using catalyst **III**.

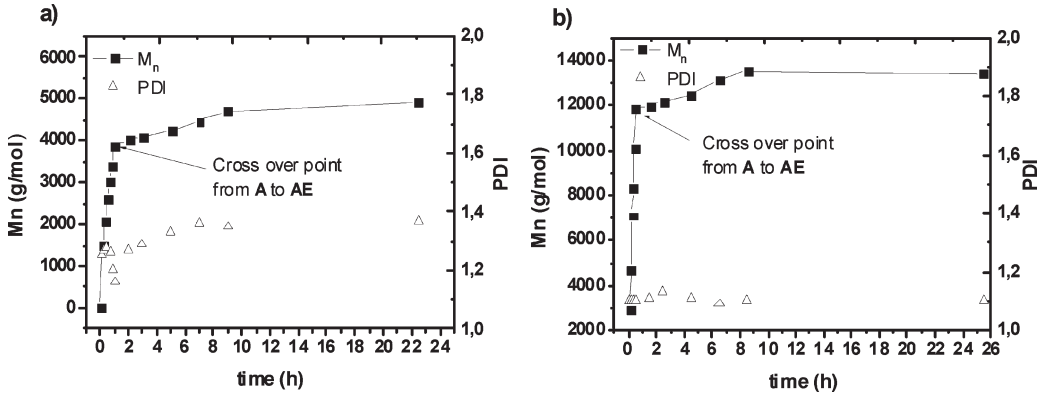


**Figure 2.** Increase in $M_{n(GPC)}$ with polymerization time ($t$) (a) for poly($\mathbf{A}_{20}$-*b*-$\mathbf{E}_{20}$) using catalyst **I** and (b) for poly($\mathbf{A}_{50}$-*b*-$\mathbf{E}_{20}$) using catalyst **III**.

**Table 1. GPC Data for Homo and Block Copolymerization of Monomer A, D, E, and T**

| sample | catalyst | $M_{n(calcd)}$ | $M_{n(GPC)}$ | $PDI_{(GPC)}$ |
|---|---|---|---|---|
| $A_{100}$ | **I** | 21 000 | 20 400 | 1.1 |
| $A_{50}$ | **III** | 10 500 | 10 800 | 1.1 |
| $A_{100}D_{100}$ | **I** | 63 500 | 53 800 | 1.2 |
| $A_{100}D_{100}$ | **III** | 63 500 | 57 000 | 1.2 |
| $A_{20}E_{20}$ | **I** | 6800 | 4900 | 1.3 |
| $A_{50}E_{20}$ | **III** | 13 100 | 13 500 | 1.1 |
| $A_{50}T_{20}$ | **III** | 20 300 | 18 200 | 1.2 |

**Table 2. Polymerization Kinetics Data Obtained from $^1$H NMR Spectroscopy**

| experiment | catalyst | $[I]_0$ (mol/L) | $k_p$ (L/mol·s$^{-1}$) | |
|---|---|---|---|---|
| $E_{20}$ | **I** | 0.02 | homo-E | 0.0045 |
| $A_{20}E_{20}$ | **I** | 0.02 | homo-A | 0.05 |
| $A_{20}E_{20}$ | **I** | 0.015 | block-E | 0.0042 |
| $E_{20}$ | **III** | 0.012 | homo-E | 0.0016 |
| $A_{20}E_{20}$ | **III** | 0.018 | homo-A | 2.60 |
| $A_{20}E_{20}$ | **III** | 0.014 | block-E | 0.0079 |
| $D_{20}$ | **I** | 0.0065 | homo-D | 2.20 |
| $A_{10}D_{10}$ | **I** | 0.015 | block-D | 1.30 |
| $D_{20}$ | **III** | 0.0066 | homo-D | 5.70 |
| $A_{20}D_{20}$ | **III** | 0.0049 | block-D | 11.90 |

spectroscopy. The extracted kinetic data ($k_p$ values) are compiled in Table 2, assuming first-order kinetics. Using Grubbs first-generation catalyst, monomer **A** is polymerized ~10 times faster than monomer **E** ($k_p$(**A**) = 0.05 L/(mol·s$^{-1}$) versus $k_p$(**E**) = 0.0045 L/(mol·s$^{-1}$)) but ~50 times slower than monomer **D** ($k_p$(**D**) = 2.2 L/(mol·s$^{-1}$)). Whereas a significant acceleration is observed when using Grubbs third-generation catalyst with monomer **A** ($k_p$(**A**) = 2.6 L/(mol·s$^{-1}$)), changes are insignificant with monomer **D** and a

**Table 3. Results for Block Copolymers Obtained by Crossover Reaction from Monomer A to Monomer D, Monomer E, and Monomer T**

| sample | catalyst | $M_{n(calcd)}$[a] | $M_{n(GPC)}$ | $PDI_{(GPC)}$ | $M_{peak(MALDI)}$[b] | $M_{n(MALDI)}$[c] | $PDI_{(MALDI)}$[d] |
|---|---|---|---|---|---|---|---|
| $A_{15}$ | **I** | 3255.4 | 2800 | 1.15 | 3280.3 | 2646.5 | 1.20 |
| $A_{15}D_1$ | **I** | 3680.5 | 3300 | 1.16 | 3494.8 | 3350.1 | 1.13 |
| $A_{15}D_4$ | **I** | 4955.7 | 3900 | 1.16 | 4556.0 | 4934.8 | 1.07 |
| $A_{15}$ | **III** | 3255.4 | 2500 | 1.13 | 2018.5 | 2250.9 | 1.07 |
| $A_{15}D_1$ | **III** | 3680.5 | 2900 | 1.18 | 3068.8 | 3888.3 | 1.09 |
| $A_{15}D_4$ | **III** | 4955.7 | 3900 | 1.14 | 4979.0 | 5878.5 | 1.06 |
| $A_{15}$ | **I** | 3255.4 | 4100 | 1.14 | 4733.4 | 4751.2 | 1.04 |
| $A_{15}E_1$ | **I** | 3385.5 | 4200 | 1.14 | 4863.3 | 4805.1 | 1.03 |
| $A_{15}E_4$ | **I** | 3775.7 | 4400 | 1.15 | 4913.4 | 4841.5 | 1.02 |
| $A_{15}$ | **III** | 3255.4 | 3600 | 1.09 | 4734.2 | 5565.1 | 1.05 |
| $A_{15}E_1$ | **III** | 3385.5 | 3800 | 1.10 | 5705.1 | 5847.7 | 1.03 |
| $A_{15}E_4$ | **III** | 3775.7 | 3900 | 1.07 | 5705.3 | 5865.4 | 1.03 |
| $A_{15}$ | **I** | 3278.4 | 3100 | 1.21 | 3911.2 | 3742.3 | 1.03 |
| $A_{15}T_1$ | **I** | 3756.7 | 3300 | 1.14 | 4538.4 | 4330.6 | 1.01 |
| $A_{15}T_2$ | **I** | 4233.0 | 3800 | 1.21 | 4537.6 | 4477.0 | 1.01 |
| $A_{15}$ | **III** | 3278.4 | 3700 | 1.09 | 4751.1 | 5256.1 | 1.04 |
| $A_{15}T_1$ | **III** | 3756.7 | 4700 | 1.10 | 5802.1 | 5842.5 | 1.02 |
| $A_{15}T_2$ | **III** | 4233.0 | 4900 | 1.08 | 6432.9 | 6580.5 | 1.02 |

[a] Calculated monoisotopic peak value including starting group (Ph), end group (vinyl), and excluding ions. [b] Peak maximum of main series from MALDI spectra. [c] Calculated average $M_n$ using Polytools software. [d] $M_w/M_n$ calculated using Polytools software.

factor of ~3 with monomer **E** ($k_p$(**D**) = 5.7 L/(mol·s$^{-1}$) and $k_p$(**E**) = 0.0016 L/(mol·s$^{-1}$)). Observing the kinetics of monomers **E** or **D**, block copolymer (initiating polymerization with a constant block of living poly($\mathbf{A}_{20}$)) does lead only to small changes of the $k_p$ values of the individual monomers, which is indicative of the fact that the presence of a homopolymer chain poly(**A**) does not induce changes in the kinetics and thus transition states during the catalytic process. The presence of residual monomer **A** before the crossover reaction was checked by $^1$H NMR spectroscopy and TLC to be below 1/100 of its starting value, thus excluding residual monomer **A** during the crossover reaction.

**Monitoring Crossover Efficiency via MALDI.** Because GPC or NMR methods cannot provide a deeper insight into the crossover reaction, we have studied this process by MALDI-TOF methods because homopolymers derived from monomer **A** can be very well desorbed and detected by MALDI methods[28] as an analytical tool for monitoring the crossover reaction. MALDI mass spectrometry enables us to monitor the analysis of copolymers,[29] mostly described via block copolymers prepared by mostly anionic[30−35] and ring-opening[36,37] polymerization processes. Therefore, the successful analysis of ROMP polymers has been described by various authors, enabling also the application to homopolymerization reactions[38] or end-capping reactions[39−41] of norbornene-based monomers. The crossover reaction was studied starting from the living poly($\mathbf{A}_{15}$) species (initiated either with Grubbs first- or third-generation catalysts) and subsequent addition of exactly 1, 2, or 4 equiv of the second monomer (**D**, **T**, **E**) with respect to the living Ru-carbene, which is similar to step-crossover experiments in living anionic polymerization processes.[42] GPC traces do show the expected shift in molecular weight with increasing amounts of the second monomer (see Supporting Information for an overlay of the GPC-curves), as is also indicated in Table 3.

In all cases, the polydispersity remains within the range of the homopolymer (~1.1 to 1.2), and the molecular weights $M_n$ increase with an increasing amount of added equivalents of monomer. Because poly($\mathbf{A}_{15}$) is an excellent probe for desorption in MALDI, the crossover reaction was monitored directly using mass spectrometry, enabling us to check the individual species due to their different masses and isotope patterns. Figures 3 and 4 show the MALDI spectra for the crossover reaction of the living homopolymer poly($\mathbf{A}_{15}$) with monomer **T** using Grubbs first- and third- generation catalysts, respectively. The crossover reaction of poly($\mathbf{A}_{15}$-*b*-$\mathbf{T}_1$) and poly($\mathbf{A}_{15}$-*b*-$\mathbf{T}_2$) using Grubbs first-generation catalyst indicates a slow crossover reaction, with significant amounts of homopolymer present even after the addition of two equiv of monomer **T**. (See Figure 3a,b.) Therefore, significant peaks assignable to **A** species without added **T**-monomers can be observed. Surprisingly the crossover reaction of poly($\mathbf{A}_{15}$-*b*-$\mathbf{T}_1$) and poly($\mathbf{A}_{15}$-*b*-$\mathbf{T}_2$) in the reaction catalyzed by Grubbs third-generation catalyst shows a similar picture (Figure 4a,b), despite the expectation that Grubbs third-generation catalyst should lead to a faster crossover reaction.

However, results are very different studying the crossover reaction between the living homopolymer poly($\mathbf{A}_{15}$) and monomer **E** in a similar experiment as described above. Again (see Table 3 and the Supporting Information), the shift in molecular weight upon the addition of 1 and 4 equiv of monomer **E** is observed via GPC using Grubbs first- and Grubbs third-generation catalysts. However, MALDI analysis (Figures 5 and 6) shows a different picture, whereas the use of Grubbs first-generation catalyst (Figure 5) still shows pure $\mathbf{A}_n$ species (i.e., $\mathbf{A}_{22}$−$\mathbf{A}_{24}$) with 1 and 4 equiv of monomer **E**; the use of Grubbs third-generation catalyst already leads to a strong reduction of the homopolymer poly($\mathbf{A}_{15}$) after the addition of 1 equiv of monomer **E**. The addition of 4 equiv of monomer **E** leads to a nearly complete crossover reaction because the poly($\mathbf{A}_n$) species are hardly detected. (See Figure 6.) Note that according to our kinetic measurements, the $k_p$ of monomer **E** does only change by a factor of ~3 when using Grubbs first- or third-generation catalysts with $k_p$(**E**) = 0.0045 and 0.0016 L/(mol·s$^{-1}$), respectively. Because $k_p$ of monomer **A** is increased significantly when changing from Grubbs first- to third-generation catalyst ($k_p$(**A**) = 0.05 vs 2.6 L/(mol·s$^{-1}$)), this is also indicative of a reactivity enhancement of the carbenes in poly(**A**) when changing from Grubbs first- to third-generation catalyst in this crossover reaction. Therefore, the largely different $k_p$ values between $k_p$(**A**)/$k_p$(**E**) = 2.60/0.0016 (catalyst **III**) and 0.05/0.0045 (catalyst **I**) can account for the more efficient crossover reaction in the case of Grubbs third-generation catalyst (catalyst **III**).

Performing the same experiment with the crossover reaction of poly($\mathbf{A}_{15}$) to monomer **D** (Figures 7 and 8), the MALDI analysis leads to the picture of a still incomplete crossover reaction even with 4 equiv of monomer **D** irrespective of the use of Grubbs first- or third-generation catalyst. Despite the fact

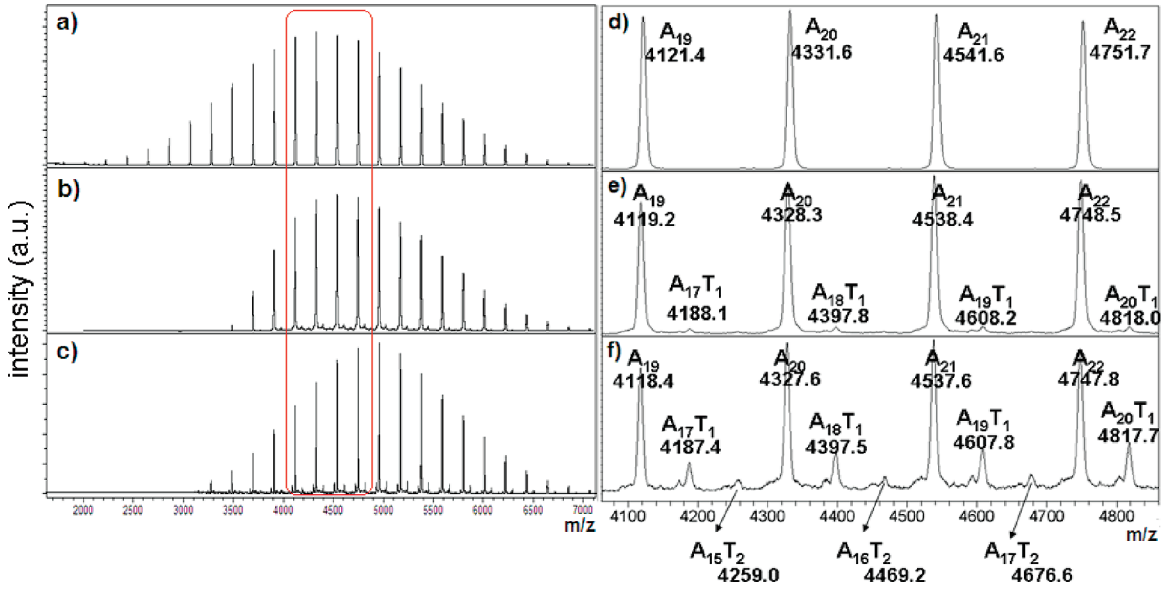


**Figure 3.** MALDI-TOF mass spectra of poly($\mathbf{A}_{15}$) ((a) complete spectra, (d) enlargement), poly($\mathbf{A}_{15}$-*b*-$\mathbf{T}_1$) ((b) complete spectra, (e) enlargement) and poly($\mathbf{A}_{15}$-*b*-$\mathbf{T}_2$) ((c) complete spectra, (f) enlargement) prepared with catalyst **I**. (All chains are desorbed as [M-$Na^+$] ions.)

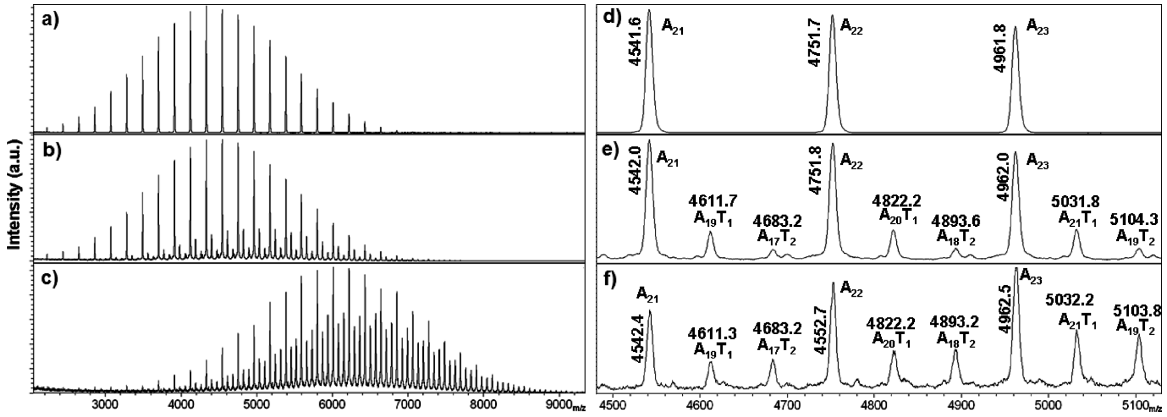


**Figure 4.** MALDI-TOF mass spectra of poly($\mathbf{A}_{15}$) ((a) full spectrum, (d) enlargement), poly($\mathbf{A}_{15}$-*b*-$\mathbf{T}_1$) ((b) full spectrum, (e) enlargement), and poly($\mathbf{A}_{15}$-*b*-$\mathbf{T}_2$) ((c) full spectrum, (f) enlargement) prepared with catalyst **III**. (All chains are desorbed as [M-$Na^+$] ions.)

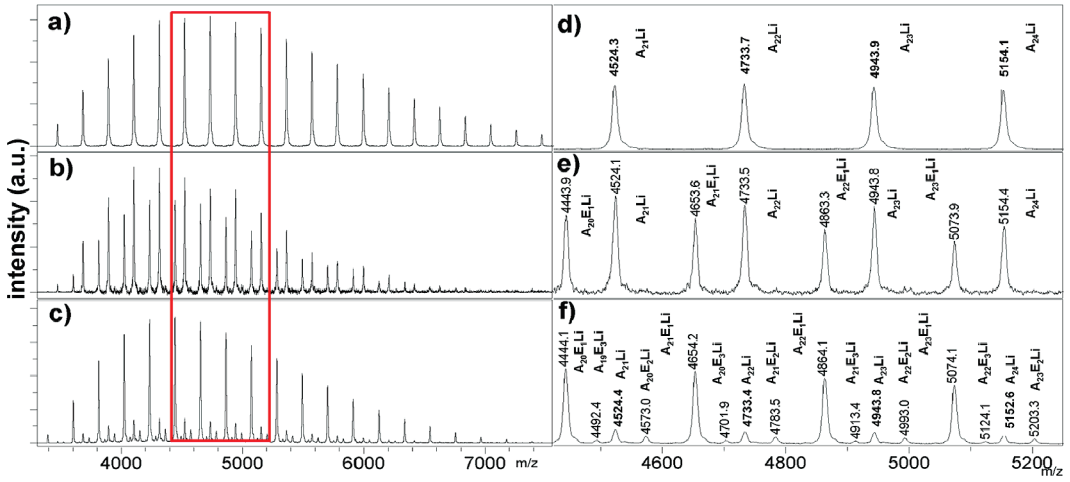


**Figure 5.** MALDI-TOF mass spectra of poly($\mathbf{A}_{15}$) ((a) complete spectra, (d) enlargement), poly($\mathbf{A}_{15}$-*b*-$\mathbf{E}_1$) ((b) complete spectra, (e) enlargement), and poly($\mathbf{A}_{15}$-*b*-$\mathbf{E}_4$) ((c) complete spectra, (f) enlargement) prepared with catalyst **I**. (All chains of the main series are desorbed as [M-$Li^+$] ions.)

that the kinetics for monomers **D** and **A** are significantly faster with Grubbs third-generation catalyst (1st-generation (**I**): $k_p$(**A**) = 0.05 and $k_p$(**D**) = 2.2 L/(mol·$s^{-1}$); third-generation (**III**): $k_p$(**A**) = 2.60 and $k_p$(**D**) = 11.90 L/(mol·$s^{-1}$)), the crossover reaction is by no means better when analyzed by the described MALDI method.

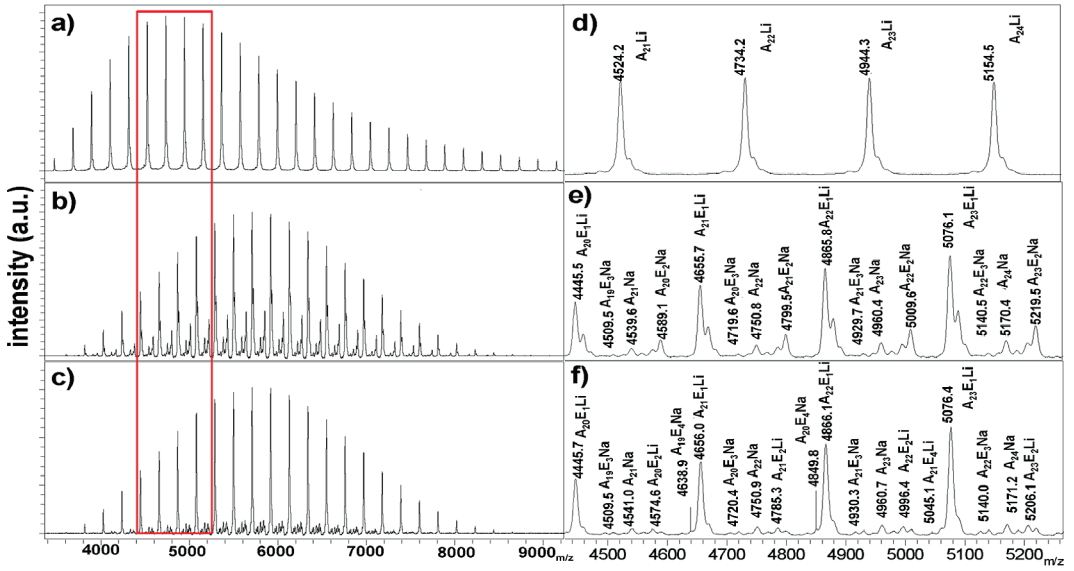


**Figure 6.** MALDI-TOF mass spectra of poly($\mathbf{A}_{15}$) ((a) complete spectra, (d) enlargement), poly($\mathbf{A}_{15}$-*b*-$\mathbf{E}_1$) ((b) complete spectra, (e) enlargement), and poly($\mathbf{A}_{15}$-*b*-$\mathbf{E}_4$) ((c) complete spectra, (f) enlargement) prepared with catalyst **III**. (Most chains of main series are desorbed as [M-Li$^+$] ions and a few are desorbed as [M-Na$^+$] ions.)

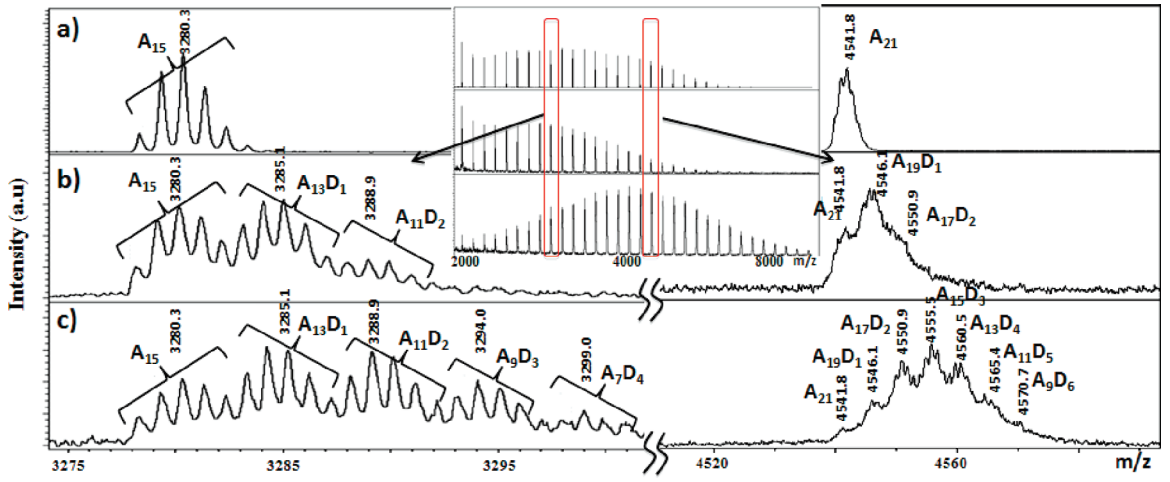


**Figure 7.** MALDI-TOF mass spectra of (a) poly($\mathbf{A}_{15}$), (b) poly($\mathbf{A}_{15}$-*b*-$\mathbf{D}_1$), and (c) poly($\mathbf{A}_{15}$-*b*-$\mathbf{D}_4$) prepared via catalyst **I**. (Insert shows the complete MALDI spectra of the samples a−c; all chains are desorbed as [M-Na$^+$] ions.)

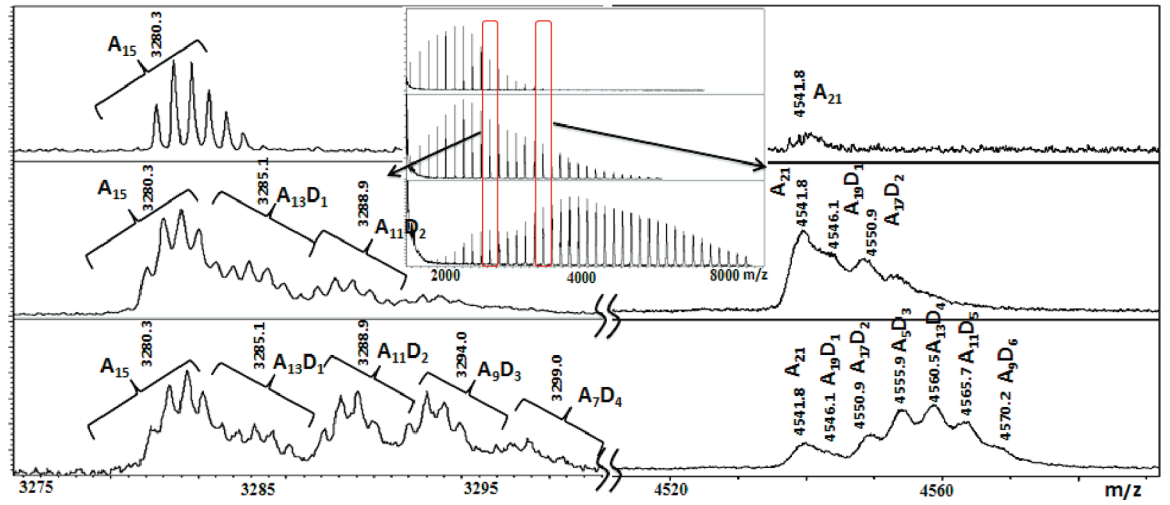


**Figure 8.** MALDI-TOF mass spectra of (a) poly($\mathbf{A}_{15}$), (b) poly($\mathbf{A}_{15}$-*b*-$\mathbf{D}_1$), and (c) poly($\mathbf{A}_{15}$-*b*-$\mathbf{D}_4$) prepared via catalyst **III**. (Insert shows the complete MALDI spectra of samples a−c; all chains are desorbed as [M-Na$^+$] ions.)

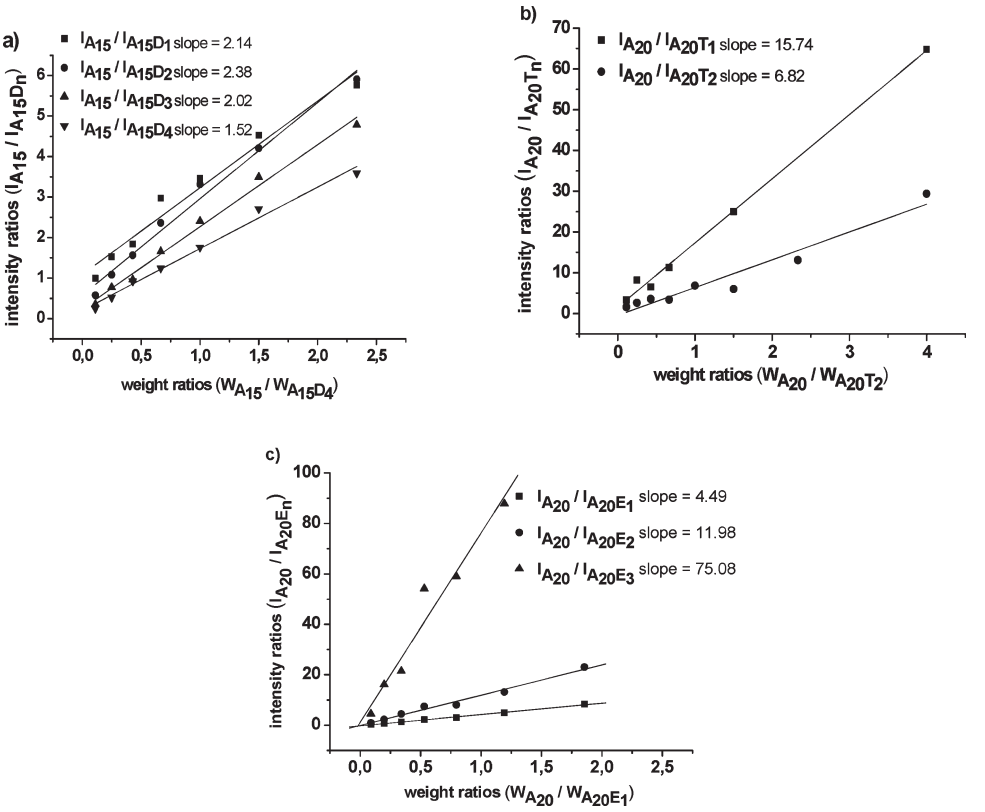


**Figure 9.** Plot of signal intensity ratios versus weight ratios (MALDI-TOF mass spectra) of (a) poly($\mathbf{A}_{15}$) and poly($\mathbf{A}_{15}$-*b*-$\mathbf{D}_4$) mixtures, (b) poly($\mathbf{A}_{15}$) and poly($\mathbf{A}_{15}$-*b*-$\mathbf{T}_2$) mixtures, and (c) poly($\mathbf{A}_{15}$) and poly($\mathbf{A}_{15}$-*b*-$\mathbf{E}_1$) mixtures. The intensities of the individual ions of poly($\mathbf{A}_{20}$-*b*-$\mathbf{X}_{1,2,3,4.}$)[$Na^+$] ions are plotted against the corresponding weight ratios, yielding the individual sensitivity values for the corresponding desorbed ions. In part c, poly($\mathbf{A}_{15}$-*b*-$\mathbf{E}_n$)[$Li^+$] ions are compared with poly($\mathbf{A}_{15}$)[$Na^+$] ions.

It is well known that MALDI analyses can hardly be quantified between polymers of different chemical structures, because desorption of even high- and low-molecular-weight species of the same type of polymer might be different.[43−47] To this purpose (Figure 9), we have measured sensitivity plots according to previous authors[44,46,48,49] by quantifying the intensity of defined physical mixtures in the final corresponding MALDI spectra. The quantities of the individual species were calculated from the individual MALDI peak intensity values, and the respective amounts of the poly($\mathbf{A}_n$-*b*-$\mathbf{X}_m$)-species ($\mathbf{X}$ = monomers **D**, **E**, and **T**) were summed up and thus quantified from the MALDI spectrum. Therefore, we have quantified the influence of chain length of the second block (X) by measuring physical poly($A_{15}$) versus poly($A_{15}$-*b*-$X_n$) mixtures ($n$ = 1, 2, 3, and 4) against the individual ions (i.e., by quantifying the poly($A_{15}$)-[$Na^+$] ion versus the poly($A_{15}$-*b*-$D_1$)-[$Na^+$] ion, poly($A_{15}$-*b*-$D_2$)-[$Na^+$] ion, poly($A_{15}$-*b*-$D_3$)-[$Na^+$] ion, and poly($A_{15}$-*b*-$D_4$)-[$Na^+$] ion). Therefore, the individual peaks of the individual ions were now selected (using the same [$Na^+$] ions as later used in the intensity checks) and then quantified against each other. The results are shown in Figure 9, which provides the sensitivities of the individual poly($A_{15}X_n$ species ($n$ = 1, 2, 3 and 4), as resolved in the MALDI. Data were evaluated by integration of the individual ions,[44] leading to sensitivity factors of the poly($A_{15}$-*b*-$D_n$) series with ($A_{15}$-*b*-$D_1$)/($A_{15}$-*b*-$D_2$)/($A_{15}$-*b*-$D_3$)/($A_{15}$-*b*-$D_4$) = 2.14/2.38/2.02/1.52, all measured in relation to the poly($A_{15}$)-[$Na^+$] ion. Therefore, the differences between the desorption of the individual poly($A_{15}$-*b*-$X_n$)-species are small, indicating that including the above measured factors, the (semi-) quantification and thus evaluation of the individual species is possible. For the other two examples (monomers **T** and **E**), the sensitivities scale as ($A_{20}$-*b*-$T_1$)/($A_{20}$-*b*-$T_2$) = 15.74/6.82 (both as [$Na^+$] ion) and I($A_{20}$-*b*-$E_1$)/($A_{20}$-*b*-$E_2$)/($A_{20}$-*b*-$E_3$) = 4.49/11.98/75.08 (all as [$Li^+$] ion), respectively. Therefore, these factors can be included in Table 4 to estimate the intensities of the individual poly($A_n$-*b*-$X_m$)-species.

On the basis of this data analysis, a rough quantification of the different species emerging directly after the corresponding crossover reactions of living poly($\mathbf{A}_{15}$) with the various monomers, based on MALDI analyses, was achieved. (See Table 4.)

The data are shown for the individual crossover experiments, listed according to the $\mathbf{A}_n$ values, with setting the intensity of the respective poly($\mathbf{A}_n$) species ($n$ = 15, 20) within one spectrum to 1.0. The values in brackets give the corresponding amounts generated by multiplying by the previously obtained sensitivity factors, thus representing the relative amounts of the individual poly($\mathbf{A}_{15}$-*b*-$\mathbf{X}_{1,2,3,4}$) species. The previously qualitatively discussed trend can thus be observed now (semi) quantitatively. Therefore, in the case of poly($\mathbf{A}_{15}$-*b*-$\mathbf{E}_n$)-experiments (Grubbs first-generation catalyst: entry 9, 10; Grubbs third-generation catalyst: entry 11, 12), low amounts of initial homopolymer−poly($\mathbf{A}_{20}$) species (i.e., species which have not participated in a crossover reaction) and high amounts of the poly($\mathbf{A}_{20}$-*b*-$\mathbf{E}_n$)-species are observed. The ratio of poly($\mathbf{A}_{20}$)/poly($\mathbf{A}_{20}$-*b*-$\mathbf{E}_1$)/poly($\mathbf{A}_{20}$-*b*-$\mathbf{E}_2$)/poly($\mathbf{A}_{20}$-*b*-$\mathbf{E}_3$) (Grubbs first-generation catalyst, entry 10) is 1.00/22.45/4.97/11.26; with Grubbs third-generation-catalyst (entry 12), the ratio is 1.00/89.80/43.12/150.15, also indicating a small amount of poly($\mathbf{A}_{20}$-*b*-$\mathbf{E}_4$)-species (2.80). Therefore, it can be concluded that the crossover reaction proceeds better with Grubbs third-generation catalyst, because the amount of poly($\mathbf{A}_{20}$) species is smaller, and the higher species poly($\mathbf{A}_{20}$-*b*-$\mathbf{E}_{1,2,3,4.}$) are present in

**Table 4. MALDI Signal Intensity Ratios of the Crossover Reactions and Corrected Intensities in Brackets[a]**

| entry | sample | X | catalyst | $n$ | $A_n$ | $A_nX_1$ | $A_nX_2$ | $A_nX_3$ | $A_nX_4$ |
|---|---|---|---|---|---|---|---|---|---|
| 1 | $A_{15}D_1$ | D | **I** | 15 | 1.00 | 1.10 (2.35) | 0.51 (1.22) | | |
| 2 | $A_{15}D_4$ | D | **I** | 15 | 1.00 | 1.55 (3.32) | 2.03 (4.83) | 2.10 (4.24) | 1.92 (2.92) |
| 3 | $A_{15}D_1$ | D | **III** | 15 | 1.00 | 0.72 (1.54) | 0.51 (1.22) | | |
| 4 | $A_{15}D_4$ | D | **III** | 15 | 1.00 | 0.53 (1.13) | 1.64 (3.90) | 1.73 (3.49) | 1.65 (2.51) |
| 5 | $A_{15}T_1$ | T | **I** | 20 | 1.00 | 0.05 (0.79) | | | |
| 6 | $A_{15}T_2$ | T | **I** | 20 | 1.00 | 0.06 (0.94) | 0.01 (0.07) | | |
| 7 | $A_{15}T_1$ | T | **III** | 20 | 1.00 | 0.24 (3.78) | 0.30 (2.05) | | |
| 8 | $A_{15}T_2$ | T | **III** | 20 | 1.00 | 0.24 (3.78) | 0.31 (2.11) | | |
| 9 | $A_{15}E_1$ | E | **I** | 20 | 1.00 | 0.69 (3.10) | | | |
| 10 | $A_{15}E_4$ | E | **I** | 20 | 1.00 | 5.00 (22.45) | 0.40 (4.79) | 0.15 (11.26) | |
| 11 | $A_{15}E_1$ | E | **III** | 20 | 1.00 | 16.66 (74.80) | 4.50 (53.91) | 0.66 (49.55) | |
| 12 | $A_{15}E_4$ | E | **III** | 20 | 1.00 | 20.00 (89.80) | 3.60 (43.12) | 2.00 (150.16) | 2.80 |

[a] Corrected intensities or the quantification number of $A_nX_m$ species calculated by multiplying the MALDI peak intensity values with the respective slopes obtained from sensitivity plots of the individual ions. (See Figure 9.)

higher amounts relative to poly(**A**$_{20}$). The lower amounts of species of the type poly(**A**$_{20}$-*b*-**E**$_{1,2}$) and higher poly(**A**$_{20}$-*b*-E$_m$) species by use of the Grubbs first-generation catalyst (entry 9, 10) in comparison to their presence upon use of Grubbs third-generation catalyst (entry 10,11) clearly demonstrate the slower crossover kinetics of Grubbs first-generation catalyst. Similar experiments with poly(**A**$_{15}$-*b*-D$_n$) (entries 1−4) show the poorer crossover reaction as the amounts of initial homopolymer poly(**A**$_{15}$) species are significantly increased relative to poly(**A**$_{15}$-*b*-**D**$_1$), both with Grubbs first- and third-generation catalysts. Even with 4 equiv of **D** (entries 2 and 4), the amount of poly(**A**$_{15}$) species is significant. The situation is more drastic with poly(**A**$_{15}$-*b*-**T**$_n$) (entries 5−8), where the amounts of homopolymer poly(**A**$_{20}$) are again comparable to those of the expected species poly(**A**$_{15}$-*b*-**T**$_n$). With all performed experiments, it should be noted (Table 1) that all block copolymers could be obtained with defined molecular weights as calculated and low polydispersities ($M_w/M_n$ < 1.25). This indicates that the point of crossover in ROMP may be very different from what kinetic data allow us to see, demonstrating the high importance of MALDI methods for the (semi-)quantitative analysis of such processes.

## Summary

The present article systematically describes crossover reactions between different monomers based on Grubbs first- and third-generation catalysts. Monomer **A** gives good results when polymerized in a classical block copolymerization process with the monomers **D**, **T**, and **E**, using Grubbs first- and third-generation catalysts with measured polydispersities of $M_w/M_n$ = 1.25 and smaller, as detected by GPC. Homopolymers poly(**A**$_{15,20}$) can be used as a probe for the detection of the crossover reaction via MALDI methods using defined amounts of equivalents of structurally related but different monomers **D**, **T**, and **E**. Kinetic analysis revealed large differences between the use of Grubbs first- and third-generation catalysts, with Grubbs third-generation catalyst being the significantly faster and more efficient catalyst during the crossover reaction. MALDI analysis revealed large differences in the quality and efficiency of the crossover process, in particular. those of the **A**−**E** versus the **A**−**D** and **A**−**T** block copolymerization process. Only the **A**−**E** crossover reaction is a fast and highly efficient process, in particular, when using Grubbs third-generation catalyst. Even with 4 equiv of monomer **D** and **T** after the crossover reaction with living poly(**A**$_{15}$), significant amounts of residual homopolymer poly(**A**$_{15}$) species are still present. Moreover, the method allows us to monitor still the crossover reaction with monomers (i.e., monomer **T**) where NMR spectroscopy is no longer applicable, revealing a clear picture of the underlying chemical process during the change of monomers on the catalyst species.

**Acknowledgment.** Grants from the DFG INST 271/249-1, INST 271/247-1, and INST 271/248-1 are gratefully acknowledged.

**Supporting Information Available:** GPC curves of crossover reactions, monomer conversion versus time plots obtained from $^1$H NMR for poly(**A**), (**D**), (**E**) and poly(**A**-*b*-**D**)and poly(**A**-*b*-**E**), procedure, tables, MALDI spectra and MALDI signal intensity ratio versus weight ratio plot for sensitivity analysis, $^1$H/$^{13}$C NMR spectra for monomers **A**, **D**, **E**, and polymers poly(**A**), poly(**D**), poly(**E**), poly(**A**-b-**D**), and poly(**A**-b-**E**). This material is available free of charge via the Internet at http://pubs.acs.org.

## References and Notes

(1) Grubbs, R. H. *Tetrahedron* **2004**, *60*, 7117–7140.
(2) Frenzel, U.; Müller, B. K. M.; Nuyken, O. In *Handbook of Polymer Synthesis*, 2nd ed.; Marcel Dekker: New York, 2004; pp 381−427.
(3) Schrock, R. R.; Hoveyda, A. H. *Angew. Chem., Int. Ed.* **2003**, *42*, 4592–4633.
(4) Sanford, M. S.; Love, J. A. In *Handbook of Metathesis*; Grubbs, R. H., Ed.; Wiley-VCH: Weinheim, Germany, 2003; pp 112−131.
(5) Buchmeiser, M. R. *Chem. Rev.* **2000**, *100*, 1565–1604.
(6) Koshravi, E. In *Handbook of Metathesis*; Grubbs, R. H., Ed.; Wiley-VCH, 2003; pp 112−131.
(7) Bielawski, C. W.; Grubbs, R. H. *Prog. Polym. Sci.* **2007**, *32*, 1–29.
(8) Matyjaszewski, K. *J. Polym. Sci., Part A: Polym. Chem.* **1993**, 995–999.
(9) Conrad, J. C.; Eelman, M. D.; Silva, J. A. D.; Monfette, S.; Parnas, H. H.; Snelgrove, J. L.; Fogg, D. E. *J. Am. Chem. Soc.* **2007**, *129*, 1024–1025.
(10) Sanford, M. S.; Ulman, M.; Grubbs, R. H. *J. Am. Chem. Soc.* **2001**, *123*, 749–750.
(11) Sanford, M. S.; Love, J. A.; Grubbs, R. H. *J. Am. Chem. Soc.* **2001**, *123*, 6543–6554.
(12) Schrodi, Y.; Pederson, R. L. *Aldrichimica Acta* **2007**, *40*, 45–52.
(13) Bornand, M.; Torker, S.; Chen, P. *Organometallics* **2007**, *26*, 3585–3596.
(14) Daniel, B.; Christina, L.; Kurt, M.; Roland, W.; Ralf, K.; Christian, S. *J. Polym. Sci., Part A: Polym. Chem.* **2008**, *46*, 4630–4635.
(15) Buchowicz, W.; Holerca, M. N.; Percec, V. *Macromolecules* **2001**, *34*, 3842–3848.
(16) Volland, M. A. O.; Adlhart, C.; Kiener, C. A.; Chen, P.; Hofmann, P. *Chem.—Eur. J.* **2001**, *7*, 4621–4632.
(17) Adlhart, C.; Chen, P. *Helv. Chim. Acta* **2000**, *83*, 2192–2196.
(18) Elgert, K.-F.; Seiler, E.; Puschendorf, G.; Ziemann, W.; Cantow, H. J. *Makromol. Chem.* **1971**, *144*, 73–83.
(19) Stubenrauch, K.; Moitzi, C.; Fritz, G.; Glatter, O.; Trimmel, G.; Stelzer, F. *Macromolecules* **2006**, *39*, 5865–5874.
(20) Katsumata, T.; Qu, J.; Shiotsuki, M.; Satoh, M.; Wada, J.; Igarashi, J.; Mizoguchi, K.; Masuda, T. *Macromolecules* **2008**, *41*, 1175–1183.
(21) Binder, W. H.; Kurzhals, S.; Pulamagatta, B.; Decker, U.; Manohar Pawar, G.; Wang, D.; Kühnel, C.; Buchmeiser, M. R. *Macromolecules* **2008**, *41*, 8405–8412.
(22) Katsumata, T.; Satoh, M.; Wada, J.; Shiotsuki, M.; Sanda, F.; Masuda, T. *Macromol. Rapid Commun.* **2006**, *27*, 1206–1211.

(23) Rubin, M.; Gevorgyan, V. *Synthesis* **2004**, *5*, 796–800.
(24) Binder, W. H.; Kluger, C.; Josipovic, M.; Straif, C. J.; Friedbacher, G. *Macromolecules* **2006**, *39*, 8092–8101.
(25) Kluger, C.; Binder, W. H. *J. Polym. Sci., Part A: Polym. Chem.* **2007**, *45*, 485–499.
(26) Binder, W. H.; Kluger, C.; Straif, C. J.; Friedbacher, G. *Macromolecules* **2005**, *38*, 9405–9410.
(27) Binder, W. H.; Kluger, C. *Macromolecules* **2004**, *37*, 9321–9330.
(28) Montaudo, G.; Samperi, F.; Montaudo, M. S. *Prog. Polym. Sci.* **2006**, *31*, 277–357.
(29) Maurizio, S. M. *Mass Spectrom. Rev.* **2002**, *21*, 108–144.
(30) Terreau, O.; Luo, L.; Eisenberg, A. *Langmuir* **2003**, *19*, 5601–5607.
(31) Wilczek-Vera, G.; Yu, Y.; Waddell, K.; Danis, P. O.; Eisenberg, A. *Macromolecules* **1999**, *32*, 2180–2187.
(32) Wilczek-Vera, G.; Yu, Y.; Waddell, K.; Danis, P. O.; Eisenberg, A. *Rapid Commun. Mass Spectrom.* **1999**, *13*, 764–777.
(33) Wilczek-Vera, G.; Danis, P. O.; Eisenberg, A. *Macromolecules* **1996**, *29*, 4036–4044.
(34) Willemse, R. X. E.; Staal, B. B. P.; Donkers, E. H. D.; van Herk, A. M. *Macromolecules* **2004**, *37*, 5717–5723.
(35) Lee, D.; Teraoka, I.; Fujiwara, T.; Kimura, Y. *Macromolecules* **2001**, *34*, 4949–4957.
(36) Huijser, S.; Staal, B. B. P.; Huang, J.; Duchateau, R.; Koning, C. E. *Angew. Chem., Int. Ed.* **2006**, *45*, 4104–4108.
(37) Meier, M. A. R.; Aerts, S. N. H.; Staal, B. B. P.; Rasa, M.; Schubert, U. S. *Macromol. Rapid Commun.* **2005**, *26*, 1918–1924.
(38) Schrock, R. R.; Gabert, A. J.; Singh, R.; Hock, A. S. *Organometallics* **2005**, *24*, 5058–5066.
(39) Hilf, S.; Grubbs, R. H.; Kilbinger, A. F. M. *J. Am. Chem. Soc.* **2008**, *130*, 11040–11048.
(40) Chang, C.; Lipian, J.; Barnes, D. A.; Seger, L.; Burns, C.; Bennett, B.; Bonney, L.; Rhodes, L. F.; Benedikt, G. M.; Lattimer, R.; Huang, S. S.; Day, V. W. *Macromol. Chem. Phys.* **2005**, *206*, 1988–2000.
(41) Scherman, O. A.; Rutenberg, I. M.; Grubbs, R. H. *J. Am. Chem. Soc.* **2003**, *125*, 8515–8522.
(42) Wilczek-Vera, G.; Yu, Y.; Waddell, K.; Danis, P. O.; Eisenberg, A. *Macromolecules* **1999**, *32*, 2180–2187.
(43) Guttman, C. M.; Flynn, K. M.; Wallace, W. E.; Kearsley, A. J. *Macromolecules* **2009**, *42*, 1695–1702.
(44) Schnöll-Bitai, I.; Hrebicek, T.; Rizzi, A. *Macromol. Chem. Phys.* **2007**, *208*, 485–495.
(45) Wetzel, S. J.; Guttman, C. M.; Girard, J. E. *Int. J. Mass Spectrom.* **2004**, *238*, 215–225.
(46) Liu, X. M.; Maziarz, E. P.; Quinn, E.; Lai, Y.-C. *Int. J. Mass Spectrom.* **2004**, *238*, 227–233.
(47) Guttman, C. M.; Wetzel, S. J.; Blair, W. R.; Fanconi, B. M.; Girard, J. E.; Goldschmidt, R. J.; Wallace, W. E.; VanderHart, D. L. *Anal. Chem.* **2001**, *73*, 1252–1262.
(48) Chen, H.; He, M. *J. Am. Soc. Mass Spectrom.* **2005**, *16*, 100–106.
(49) Chen, H.; He, M.; Pei, J.; He, H. *Anal. Chem.* **2003**, *75*, 6531–6535.